JTE HCM-UTE
ISSN: 2615-9740

JOURNAL OF TECHNICAL EDUCATION SCIENCE
Ho Chi Minh City University of Technology and Engineering
Website: https://jte.edu.vn
Email: jte@hcmute.edu.vn

Synthesis of Fe Modified SnO_2 Photocatalysts for Enhanced Photocatalytic Degradation of Eosin Y Under Visible Light

Khanh Mai Quach, Tuyen Nguyen Ngoc Lam, Nhu Vo Thi Thu*
Ho Chi Minh City University of Technology and Engineering, Vietnam

*Corresponding author. Email: nhuvtt@hcmute.edu.vn

ARTICLE INFO

Received: 22/09/2026
Revised: 15/11/2026
Accepted: 23/11/2026
Online first: 27/11/2026
Published: 28/11/2026

KEYWORDS

Fe modified SnO_2;
Co-precipitation;
Photocatalyst;
Eosin Y;
Visible-light.

ABSTRACT

Fe-modified SnO_2 nanoparticles were prepared via a facile co-precipitation method and investigated as visible-light-responsive photocatalysts for the degradation of Eosin Y (EY) in aqueous solution. SnO_2 and Fe-modified SnO_2 samples containing 0.5, 1.0, 1.5, and 2.0 wt.% Fe was prepared and characterized by X-ray diffraction (XRD), field-emission scanning electron microscopy (FESEM), energy-dispersive X-ray spectroscopy (EDX), and UV–Vis diffuse reflectance spectroscopy (DRS). XRD analysis confirmed that all samples retained the tetragonal rutile structure of SnO_2, with no detectable crystalline Fe-containing secondary phases. FE-SEM revealed quasi-spherical nanoparticles with particle sizes of approximately 20–50 nm, while EDX confirmed the presence of Fe in the modified samples. Fe incorporation substantially enhanced the visible-light absorption of SnO_2, with the apparent optical band-gap energy decreasing from 3.64 eV for pristine SnO_2 to 3.04, 2.93, 2.90, and 2.86 eV for $Fe0.5/SnO_2$, $Fe1.0/SnO_2$, $Fe1.5/SnO_2$, and $Fe2.0/SnO_2$, respectively. Photocatalytic experiments demonstrated that Fe modification significantly enhanced EY degradation compared with pristine SnO_2. The enhanced photocatalytic activity is attributed primarily to the improved visible-light absorption and the modification of the electronic and defect structure of SnO_2 by Fe incorporation.

DOI: https://doi.org/10.54644/jte.2026.2622

Copyright © JTE. This is an open access article distributed under the terms and conditions of the Creative Commons Attribution-NonCommercial 4.0 International License which permits unrestricted use, distribution, and reproduction in any medium for non-commercial purpose, provided the original work is properly cited.

1. Introduction

Dye contamination of water is currently recognized as one of the major environmental concerns [1], [2]. A distinctive characteristic of synthetic dyes is their complex chemical structures, which make most dyes highly stable and resistant to degradation. Once released into water bodies, dyes can readily cause widespread water pollution and exert adverse effects on human health and aquatic organisms that depend on these water resources [3], [4]. Toxicological studies have shown that even at relatively low concentrations, dyes can cause significant toxicity to aquatic organisms, mainly because potentially harmful chemicals may be released during their slow degradation through oxidation, hydrolysis, physical interactions, and chemical reactions. In addition, dyes can hinder light penetration through aquatic systems and reduce photosynthetic activity, thereby adversely affecting aquatic life. Furthermore, some dyes may pose toxicological risks to humans, animals, and aquatic organisms because of their potential carcinogenic and mutagenic effects [5]–[7]. Therefore, from both environmental and public-health perspectives, the effective removal of dyes from water and wastewater is a high priority for protecting human health and aquatic ecosystems. However, the treatment of dye-contaminated water remains a major challenge because of the high stability of these compounds toward chemical and biological degradation processes [6], [8].

Various methods, including biological, physical, and advanced oxidation processes (AOPs), have been employed for the degradation and removal of dyes from textile wastewater. Biological methods are widely used because of their economic advantages; however, their reaction rates are generally slow, and complete removal or degradation of dyes is often difficult to achieve. Similarly, physical methods

such as adsorption, flocculation, precipitation, reverse osmosis, and coagulation may effectively remove dyes from the aqueous phase, but they do not necessarily destroy the pollutant molecules and may generate secondary waste streams [9]–[16]. In contrast, AOPs have shown considerable promise for the degradation of dyes in wastewater. A key advantage of AOPs is their relatively non-selective oxidation capability, which enables the degradation of organic pollutants through the generation of reactive hydroxyl radicals (•OH). These radicals can rapidly react with organic compounds, break down the complex molecular structures of dyes into smaller intermediates, and potentially promote their further degradation toward less harmful products. In heterogeneous photocatalysis, the photocatalyst is typically a solid semiconductor, such as titanium dioxide (TiO_2), tin dioxide (SnO_2), or other metal oxides, while the reactants are present in the liquid or gas phase. The photocatalytic process involves light absorption by the semiconductor, followed by the generation of electron–hole pairs and subsequent oxidation–reduction reactions with species adsorbed on the photocatalyst surface [17], [18].

Among semiconductor photocatalysts, SnO_2 is particularly attractive because of its stability, low toxicity, and ability to form heterojunctions that can enhance photocatalytic activity [19]. However, its relatively wide band-gap energy (Eg ≈ 3.6 eV) and rapid electron–hole recombination significantly limit its photocatalytic performance under sunlight. To overcome these limitations, researchers have increasingly investigated the incorporation of transition metals into SnO_2 [20]. This approach can modify the electronic structure of SnO_2, tune its band-gap energy, extend light absorption into the visible region, and promote the formation of oxygen vacancies. These effects can facilitate charge separation, suppress electron–hole recombination, and consequently improve photocatalytic performance [17], [20]. Among transition-metal modifiers, Fe is particularly attractive because Fe species can alter the structural and optical properties of SnO_2 and potentially improve its response to visible light [20]. Eosin Y (EY) is widely used in textile and printing applications, as well as in cosmetics and biomedical fields. Owing to its relatively stable chemical structure, EY can be persistent and difficult to naturally degrade in aqueous environments [21]. Besides, Eosin Y is an environmental contaminant and toxicant for humans. Previous studies have reported its detrimental effects on eyes, particularly the cornea and retinal ganglion cells [22]. Its exposure has also been implicated in DNA damage in gastrointestinal organs, which play a role in a range of disease conditions [23], [24]. Furthermore, by following ingestion, the Eosin Y adversely affects vital organs, notably the liver and kidneys [22], [25]. Given the bromo-substituted xanthene structure and its high chemical stability, the treatment of Eosin Y-containing wastewater often relies on advanced oxidation processes (AOPs) rather than conventional biological treatment methods [26]. Degradation products may retain toxicological activity and, in certain cases, exhibit carcinogenic potential [27].

In this context, the present study aimed to synthesize SnO_2 nanoparticles (NPs) and Fe-modified SnO_2 NPs using a simple co-precipitation method and to evaluate their photocatalytic performance toward the degradation of Eosin Y in aqueous solution under visible-light irradiation. The study specifically focused on clarifying the effect of Fe modification on the photocatalytic activity of SnO_2 and assessing its potential for enhancing visible-light-driven dye degradation. Therefore, the degradation of Eosin Y provides not only a practical model for evaluating the applicability of the prepared photocatalysts in dye-contaminated wastewater treatment but also a basis for understanding the potential of Fe-modified SnO_2 as a visible-light-responsive photocatalytic material.

2. Materials and Methods

2.1. Materials

All chemicals and reagents used for the synthesis of the photocatalysts and photocatalytic experiments were of analytical grade. Iron (III) chloride hexahydrate ($FeCl_3.6H_2O$, 99%), hydrochloric acid (HCl, 36%) and sodium hydroxide (NaOH, 99%) were purchased from Xilong Chemical (China). Tin (IV) chloride pentahydrate ($SnCl_4.5H_2O$, 99%), aqueous ammonia (NH_4OH, 25%), and Eosin Y (EY) were supplied by JHD Chemical (China). Distilled water was used throughout the synthesis and photocatalytic experiments.

2.2. Synthesis of photocatalysts

2.2.1. Synthesis of SnO_2 NPs

SnO_2 nanoparticles were synthesized using a facile co-precipitation method. Briefly, 6.0 g of $SnCl_4 \cdot 5H_2O$ was dissolved in 50 mL of distilled water under continuous magnetic stirring to obtain a homogeneous precursor solution. Aqueous NH_4OH was subsequently added dropwise under vigorous stirring until the solution reached pH 7, resulting in the formation of a precipitate. The suspension was then aged under continuous stirring for 2 hours. The resulting precipitate was collected by centrifugation and repeatedly washed with distilled water to remove residual soluble species. The washed precipitate was dried at 100 ℃ for 2 hours and subsequently calcined in air at 600 ℃ for 3 hours. The resulting material was denoted as SnO_2. A schematic illustration of the synthesis procedure is presented in Figure 1.

2.2.2. Synthesis of Fe-modified SnO_2 NPs

Fe-modified SnO_2 nanoparticles were synthesized via a co-precipitation route. First, 6.0 g of $SnCl_4 \cdot 5H_2O$ was dissolved in 50 mL of distilled water under continuous stirring. Separately, 0.0620, 0.1240, 0.1860, and 0.2480 g of $FeCl_3 \cdot 6H_2O$ were dissolved individually in 10 mL of distilled water to obtain Fe doping levels of 0.5, 1.0, 1.5, and 2.0 wt%, respectively. The Fe^{3+} precursor solution was then added to the Sn^{4+} precursor solution and stirred at room temperature for 30 min to ensure adequate mixing. Aqueous NH_4OH was subsequently added slowly until pH 7 was reached. The resulting suspension was maintained under continuous stirring for an additional 2 hours. The precipitate was then centrifuged and repeatedly washed with distilled water until a constant washing pH was obtained. The recovered precipitate was dried at 100 ℃ for 2 hours and calcined at 600 ℃ for 3 hours using a heating rate of 5 ℃ min^{-1} to obtain Fe/SnO_2. The resulting samples were denoted as $Fe0.5/SnO_2$, $Fe1.0/SnO_2$, $Fe1.5/SnO_2$, and $Fe2.0/SnO_2$, respectively.

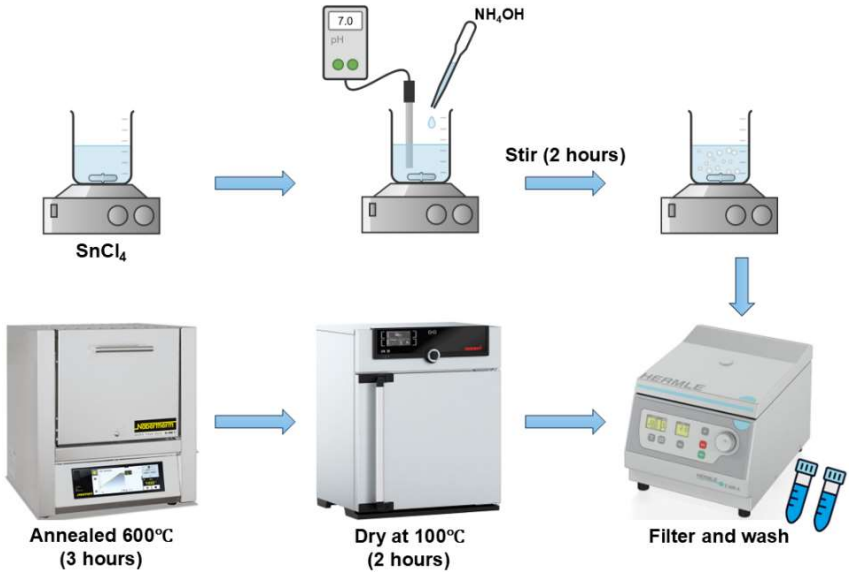


Figure 1. *Schematic diagram of the synthesis of SnO_2.*

2.3. Characterization

The structures of the synthesized materials were determined by X-ray diffraction (XRD) using a Panalytical Empyrean diffractometer with Cu Kα radiation (λ = 0.15406 nm), over a 2θ range of 10–80°. The morphology of the samples were characterized by field-emission scanning electron microscopy (FE-SEM) using an S-4800 microscope at an accelerating voltage of 10 kV, and elemental composition of of the samples were characterized by energy-dispersive X-ray spectroscopy (EDX) using Brucker

Quantax 75. UV–Vis diffuse reflectance spectra (DRS) were recorded using a V-770 Jasco spectrophotometer in the wavelength range of 200–800 nm.

2.4. Photocatalytic activity

The photocatalytic activities of pristine SnO_2 and Fe-modified SnO_2 samples, including Fe0.5/SnO_2, Fe1.0/SnO_2, Fe1.5/SnO_2, and Fe2.0/SnO_2, were evaluated by monitoring the degradation of Eosin Y (EY) under LED irradiation. For photocatalytic experiment, 0.10 g of catalyst was dispersed in 50 mL of an aqueous EY solution with an initial concentration of 50 ppm, corresponding to a catalyst loading of 2.0 g L^{-1}. Firstly, the suspension was stirred 30 min in the dark to establish adsorption–desorption equilibrium. Then the suspension was subsequently irradiated under continuous stirring for 30, 60, 90, and 120 min. At predetermined irradiation intervals, aliquots were withdrawn, centrifuged, and filtered to remove catalyst particles. The residual EY concentration was determined using UV–Vis spectroscopy at λ_{max} = 517 nm.

The reusability of the Fe/SnO_2 photocatalyst was evaluated over four photocatalytic cycles. After each cycle, the Fe/SnO_2 catalyst was recovered by centrifugation, thoroughly washed with distilled water, and dried at 100 °C before being reused in the subsequent cycle.

The EY degradation efficiency (DE) was calculated as:

$$DE(\%) = \frac{C_0 - C_t}{C_0} \times 100\% \quad (1)$$

C_o and C_t: initial EY concentration and remaining EY concentration after irradiation for time t

3. Results and Discussion

3.1. Catalyst properties

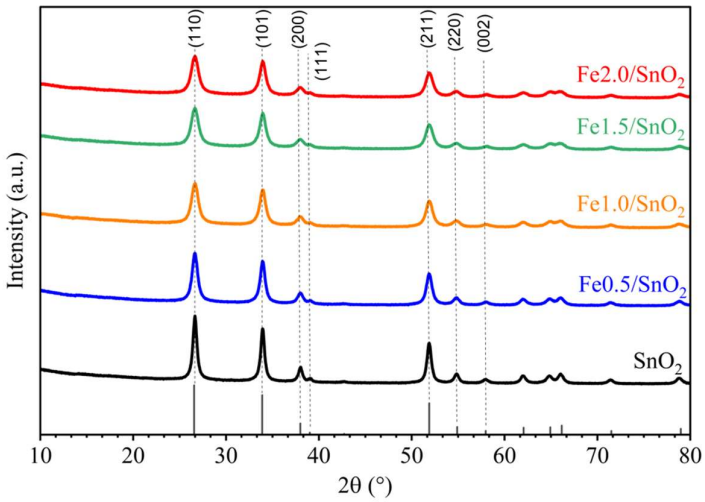


Figure 2. *XRD patterns of SnO_2 and Fe/SnO_2 NPs.*

The XRD patterns of pristine SnO_2 and Fe0.5/SnO_2, Fe1.0/SnO_2, Fe1.5/SnO_2, and Fe2.0/SnO_2 are presented in Figure 2. All samples exhibited diffraction peaks at approximately 2θ = 26.6°, 33.9°, 37.9°, 51.8°, 54.7°, 57.8°, 61.9°, 64.8°, 66.1°, 71.3°, and 78.8°, which can be indexed to the (110), (101), (200), (211), (220), (002), (310), (112), (301), (202), and (321) crystallographic planes, respectively. These reflections are characteristic of the tetragonal rutile structure of SnO_2 and are consistent with the standard diffraction data reported in JCPDS No. 41-1445 [28]. No additional diffraction peaks attributable to crystalline Fe-containing phases were detected. This observation indicates that Fe modification did not result in the formation of detectable crystalline secondary phases and that the tetragonal SnO_2 structure was retained after Fe incorporation.

The crystal size, presented in Table 1, was calculated from the (110) diffraction peak using the Scherrer formula:

$$d = \frac{0.9\lambda}{\beta \cos\theta} \quad (2)$$

With λ = 0.15406 nm, β is the half-peak width (rad), θ is the diffraction angle (°)

Compared with pure SnO_2, the Fe-modified samples exhibited changes in interplanar spacing, which can be attributed to the incorporation of Fe^{3+} into or interaction with the SnO_2 lattice, resulting in changes in lattice distortion and defect density. Thus, Fe modification affects the structural characteristics of SnO_2 while maintaining its main rutile phase, consistent with previous reports [29], [30].

Table 1. *The crystal size of pure SnO_2 and Fe/SnO_2 nanoparticles.*

Samples	2θ (°)	β (rad)	d (nm)
SnO_2	26.65	0.59106	13.85
Fe0.5/SnO_2	26.60	0.58815	14.91
Fe1.0/SnO_2	26.59	0.49317	16.62
Fe1.5/SnO_2	26.61	0.52511	15.59
Fe2.0/SnO_2	26.57	0.41242	17.85

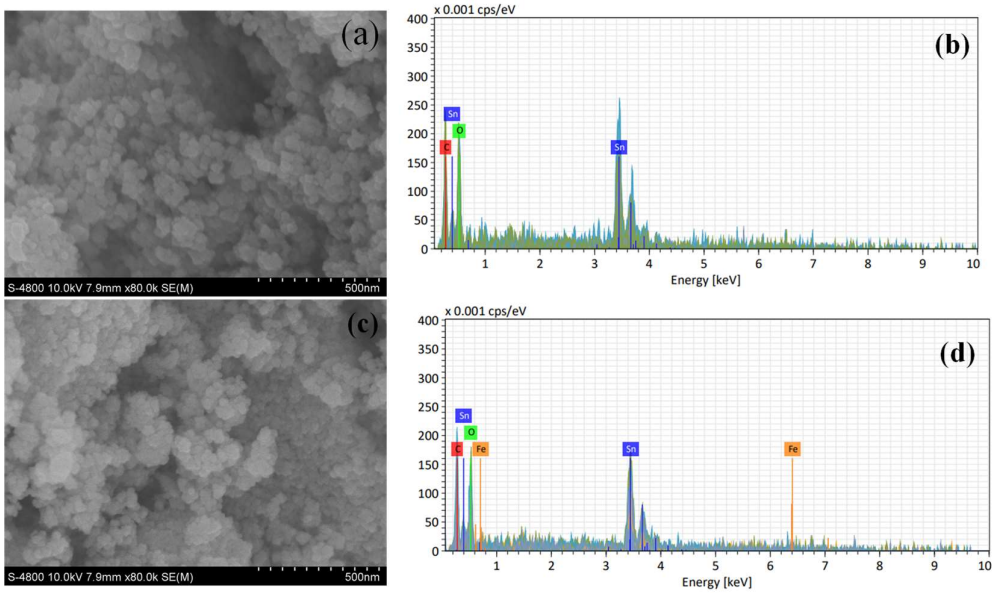


Figure 3. *FESEM image and EDX analysis of SnO_2 (a, b) and Fe1.5/SnO_2 (c, d).*

The surface morphologies of pristine SnO_2 and Fe1.5/SnO_2 are shown in Figure 3a and 3c. Both samples consisted predominantly of quasi-spherical nanoparticles with relatively homogeneous morphological distributions. The particle sizes of SnO_2 and Fe1.5/SnO_2 were approximately 20–50 nm. However, the nanoparticles exhibited a tendency to form agglomerated clusters. Such aggregation is commonly observed in nanoscale materials and can be attributed to their high surface energy, which promotes particle–particle interactions and reduces the overall surface free energy of the system. Despite the observed aggregation, interparticle voids and gaps remained visible throughout the samples. These structural features may provide accessible surface regions for pollutant adsorption and facilitate

interactions between the catalyst surface and aqueous dye molecules, which can be beneficial for photocatalytic reactions.

The elemental compositions of the synthesized materials were further examined by EDX analysis (Figure 3b and 3d). The EDX spectrum of Fe1.5/SnO_2 revealed signals corresponding to Sn, O, and Fe, confirming the presence of Fe in the Fe-modified material. In contrast, only Sn and O were detected in pristine SnO_2. The EDX results therefore provide evidence for the successful introduction of Fe-containing species during the synthesis process.

The UV–Vis diffuse reflectance spectra of pristine SnO_2 and Fe-modified SnO_2 samples are shown in Figure 4a. Pristine SnO_2 exhibited strong absorption primarily in the ultraviolet region, consistent with its wide-band-gap nature. In contrast, Fe-modified SnO_2 samples showed an extension of light absorption toward the visible region. The progressive shift in the absorption edge with increasing Fe content indicates that Fe modification altered the optical response of SnO_2.

The optical band-gap energies (Eg) were estimated from the diffuse reflectance data using the Tauc relationship:

$$\alpha h\nu = A\left(h\nu - E_g\right)^n \tag{3}$$

Where n equals 1/2 for the direct allowed transition, hυ is the photon energy, α is the absorption coefficient, and A is a constant. The Kubelka–Munk function was used to convert the diffuse reflectance data, and the band gap values were determined from the corresponding Tauc plots (Figure 4b).

The estimated band-gap energies were 3.64, 3.04, 2.93, 2.90, and 2.86 eV for SnO_2, Fe0.5/SnO_2, Fe1.0/SnO_2, Fe1.5/SnO_2, and Fe2.0/SnO_2, respectively. The progressive decrease in the apparent band-gap energy following Fe incorporation suggests the introduction of additional electronic states associated with Fe species and/or defect states within the SnO_2 electronic structure. Consequently, the modified materials can absorb a broader portion of the incident visible-light spectrum. Fe-related electronic states may also influence the migration and recombination behavior of photogenerated charge carriers. Overall, the DRS results demonstrate that Fe modification substantially altered the optical properties of SnO_2 and extended its light absorption toward the visible region.

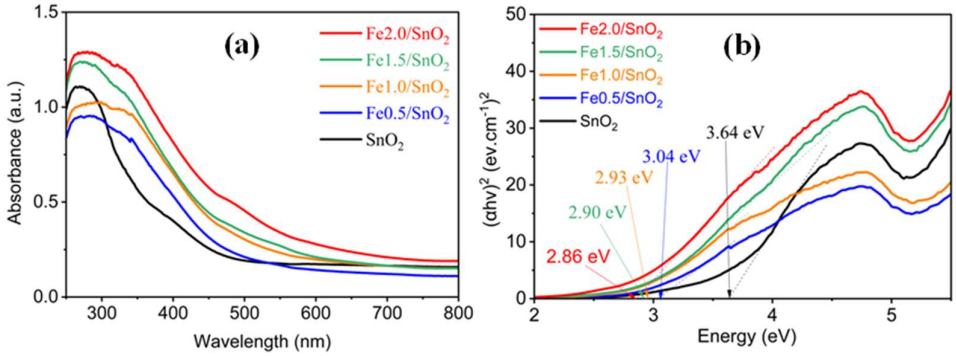


Figure 4. *(a) DRS and (b) band gap of SnO_2 and Fe/SnO_2 catalysts.*

3.2. Photocatalytic study

3.2.1. Comparison of Eosin Y photodegradation by SnO_2 and Fe/SnO_2 catalyst

The photocatalytic degradation performances of pristine SnO_2 and Fe-modified SnO_2 toward Eosin Y are presented in Figure 5. The experiments were conducted using an initial EY concentration of 50 ppm and a catalyst dosage of 2.0 g L^{-1}. The blank experiment showed negligible EY degradation in the absence of a photocatalyst, indicating that direct photolysis under the applied irradiation conditions was limited. After 120 min of irradiation, pristine SnO_2 achieved an EY degradation efficiency of 41.67%. In comparison, Fe-modified SnO_2 exhibited degradation efficiencies of 87.82%, 87.50%, 94.58%, and 61.98% for Fe0.5/SnO_2, Fe1.0/SnO_2, Fe1.5/SnO_2, and Fe2.0/SnO_2, respectively. Fe1.5/SnO_2 exhibited the highest degradation efficiency among the investigated samples, reaching 94.58% after 120 min. The

enhanced photocatalytic performance following Fe modification can be associated with the altered optical properties and the possible involvement of Fe-related electronic or defect states. Nevertheless, the lower activity observed for the 2.0 wt.% Fe sample indicates that increasing the Fe content beyond an optimum level does not necessarily result in further enhancement. Excessive Fe incorporation may introduce additional recombination centers, alter surface properties, or reduce the availability of catalytically active sites. Thus, the photocatalytic performance depended strongly on the Fe content, with Fe1.5/SnO_2 exhibiting the highest activity under the investigated conditions.

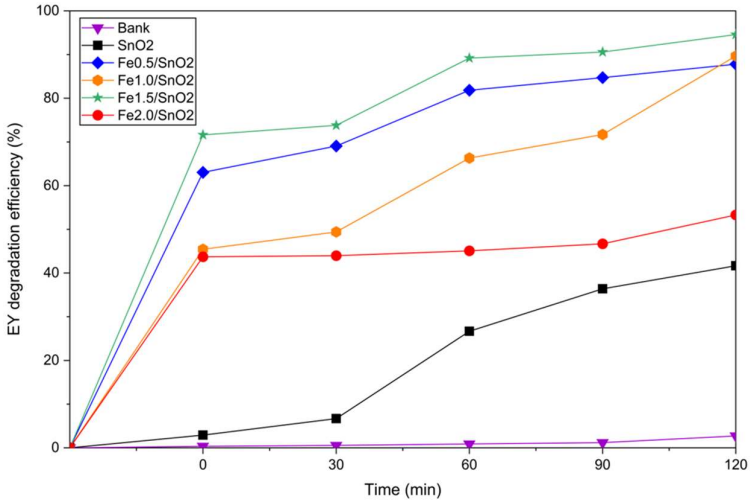


Figure 5. *EY degradation efficiency of SnO_2 and Fe/SnO_2 catalysts.*

3.2.2. Reusability

The stability and reusability of the 1.5%Fe/SnO_2 catalyst were evaluated through four consecutive photocatalytic cycles for Eosin Y degradation. As shown in Figure 6, the degradation efficiency gradually decreased after each reuse. After 120 min of irradiation, the degradation efficiencies in the first, second, third, and fourth cycles were 94.45%, 88.26%, 85.08%, and 72.45%, respectively. The decrease in photocatalytic activity may be attributed to the adsorption of residual Eosin Y molecules and intermediate products on the catalyst surface. Although the catalyst was recovered and washed after each cycle, some adsorbed species may remain on the surface, blocking active sites and reducing light accessibility and contact between the pollutant and catalyst.

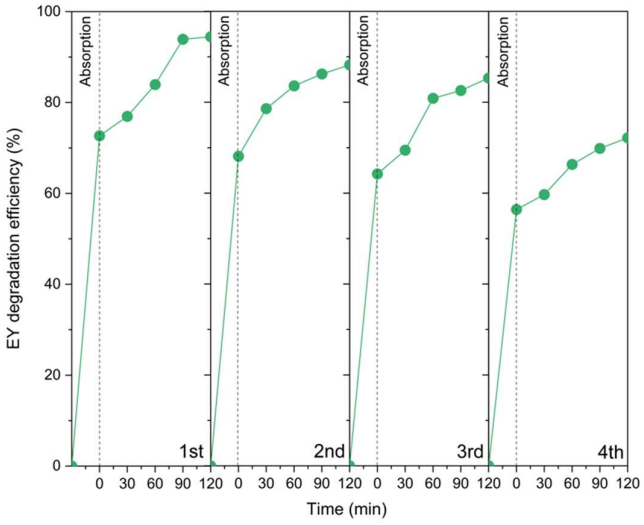


Figure 6. *EY degradation efficiency of Fe1.5/SnO_2 catalyst after four reuses.*

4. Conclusions

SnO_2 and Fe/SnO_2 nanomaterials with different Fe contents were successfully synthesized by the co-precipitation method. XRD analysis confirmed that all samples retained the characteristic tetragonal rutile structure of SnO_2 without the appearance of new crystalline phases, indicating that Fe doping did not alter the basic crystal structure of SnO_2. The incorporation of Fe significantly reduced the optical band gap of SnO_2 from 3.64 eV to 2.86 eV, thereby enhancing its visible-light absorption. The photocatalytic activity of the synthesized materials was evaluated through the degradation of 50 ppm Eosin Y under visible-light irradiation. All Fe/SnO_2 samples exhibited higher degradation efficiencies than pristine SnO_2, with Fe1.5/SnO_2 achieving the highest efficiency of 94.58% after 120 min of irradiation. This result demonstrates that Fe modification can significantly improve the photocatalytic performance of SnO_2. The reusability test further showed that the catalyst maintained its photocatalytic activity after three consecutive cycles, indicating relatively good stability and potential for application in dye-containing wastewater treatment.

Acknowledgments

The authors would like to sincerely thank Ho Chi Minh City University of Technology and Engineering, Vietnam, for supporting the necessary apparatus and equipment for the experiment.

Conflict of Interest

The authors declare no conflict of interest.

Declaration of generative AI and AI-assisted technologies in the writing process

During the preparation of this work, the authors used ChatGPT in order to English language editing. After using this tool/service, the authors reviewed and edited the content as needed and take full responsibility for the publication's content.

REFERENCES

[1] J. Lin *và c.s.*, "Environmental impacts and remediation of dye-containing wastewater", *Nat Rev Earth Environ*, tập 4, số 11, tr 785–803, thg. 11 2023, doi: 10.1038/s43017-023-00489-8.
[2] M. Tripathi *và c.s.*, "Recent Strategies for the Remediation of Textile Dyes from Wastewater: A Systematic Review", *Toxics*, tập 11, số 11, tr 940, thg. 11 2023, doi: 10.3390/toxics11110940.
[3] L. Zhang, X. Zhou, X. Guo, X. Song, và X. Liu, "Investigation on the degradation of acid fuchsin induced oxidation by $MgFe_2O_4$ under microwave irradiation", *Journal of Molecular Catalysis A: Chemical*, tập 335, số 1, tr 31–37, thg. 2 2011, doi: 10.1016/j.molcata.2010.11.007.
[4] M. T. Yagub, T. K. Sen, S. Afroze, và H. M. Ang, "Dye and its removal from aqueous solution by adsorption: A review", *Advances in Colloid and Interface Science*, tập 209, tr 172–184, thg. 7 2014, doi: 10.1016/j.cis.2014.04.002.
[5] H. R. Mahmoud, S. A. El-Molla, và M. Saif, "Improvement of physicochemical properties of Fe_2O_3/MgO nanomaterials by hydrothermal treatment for dye removal from industrial wastewater", *Powder Technology*, tập 249, tr 225–233, thg. 11 2013, doi: 10.1016/j.powtec.2013.08.021.
[6] M. R. Joya, J. Barón-Jaimez, và J. Barba-Ortega, "Preparation and characterization of Fe_2O_3 nanoparticles", *J. Phys.: Conf. Ser.*, tập 466, tr 012004, thg. 11 2013, doi: 10.1088/1742-6596/466/1/012004.
[7] D. Mehta, S. Mazumdar, và S. K. Singh, "Magnetic adsorbents for the treatment of water/wastewater—A review", *Journal of Water Process Engineering*, tập 7, tr 244–265, thg. 9 2015, doi: 10.1016/j.jwpe.2015.07.001.
[8] S. Kumari, D. Mankotia, và G. S. Chauhan, "Crosslinked cellulose dialdehyde for Congo red removal from its aqueous solutions", *Journal of Environmental Chemical Engineering*, tập 4, số 1, tr 1126–1136, thg. 3 2016, doi: 10.1016/j.jece.2016.01.008.
[9] K. K. Kefeni và B. B. Mamba, "Photocatalytic application of spinel ferrite nanoparticles and nanocomposites in wastewater treatment: Review", *Sustainable Materials and Technologies*, tập 23, tr e00140, thg. 4 2020, doi: 10.1016/j.susmat.2019.e00140.
[10] M. Kadhom, N. Albayati, H. Alalwan, và M. Al-Furaiji, "Removal of dyes by agricultural waste", *Sustainable Chemistry and Pharmacy*, tập 16, tr 100259, thg. 6 2020, doi: 10.1016/j.scp.2020.100259.
[11] A. K. Jain, V. K. Gupta, A. Bhatnagar, và Suhas, "Utilization of industrial waste products as adsorbents for the removal of dyes", *Journal of Hazardous Materials*, tập 101, số 1, tr 31–42, thg. 7 2003, doi: 10.1016/S0304-3894(03)00146-8.
[12] H. Liu, J. Zhang, M. Lu, L. Liang, H. Zhang, và J. Wei, "Biosynthesis based membrane filtration coupled with iron nanoparticles reduction process in removal of dyes", *Chemical Engineering Journal*, tập 387, tr 124202, thg. 5 2020, doi: 10.1016/j.cej.2020.124202.
[13] K. Jankowska, Z. Su, J. Zdarta, T. Jesionowski, và M. Pinelo, "Synergistic action of laccase treatment and membrane filtration during removal of azo dyes in an enzymatic membrane reactor upgraded with electrospun fibers", *Journal of Hazardous Materials*, tập 435, tr 129071, thg. 8 2022, doi: 10.1016/j.jhazmat.2022.129071.
[14] M. M. Hassan và C. M. Carr, "A critical review on recent advancements of the removal of reactive dyes from dyehouse effluent by ion-exchange adsorbents", *Chemosphere*, tập 209, tr 201–219, thg. 10 2018, doi: 10.1016/j.chemosphere.2018.06.043.
[15] K. Selvam, K. Swaminathan, và K.-S. Chae, "Decolourization of azo dyes and a dye industry effluent by a white rot fungus *Thelephora* sp.", *Bioresource Technology*, tập 88, số 2, tr 115–119, thg. 6 2003, doi: 10.1016/S0960-8524(02)00280-8.
[16] L. Y. Jun *và c.s.*, "An overview of immobilized enzyme technologies for dye and phenolic removal from wastewater", *Journal of Environmental Chemical Engineering*, tập 7, số 2, tr 102961, thg. 4 2019, doi: 10.1016/j.jece.2019.102961.

[17] P. V. Jithin, K. Sudheendran, K. J. Sankaran, và J. Kurian, "Influence of Fe-doping on the structural and photoluminescence properties and on the band-gap narrowing of SnO2 nanoparticles", *Optical Materials*, tập 120, tr 111367, thg. 10 2021, doi: 10.1016/j.optmat.2021.111367.
[18] F. Zhan *và c.s.*, "A comprehensive review of oxygen vacancy modified photocatalysts: synthesis, characterization, and applications", *Phys. Chem. Chem. Phys.*, tập 26, số 15, tr 11182–11207, thg. 4 2024, doi: 10.1039/d3cp06126d.
[19] J. R. Sunkara và S. M. Botsa, "SnO_2/Fe_2O_3/Ag Nanocomposite via Hydrothermal Approach: A Novel Highly Efficient Photodegradation of Eosin Yellow and Brilliant Green Dyes Under Visible Light Irradiation", *Chemistry Africa*, tập 2, số 4, tr 635–644, thg. 12 2019, doi: 10.1007/s42250-019-00086-7.
[20] A. B. Ali Baig, V. Rathinam, và V. Ramya, "Synthesis and Investigation of Fe doped SnO_2 Nanoparticles for Improved Photocatalytic Activity under Visible Light and Antibacterial performances", *Materials Technology*, tập 36, số 10, tr 623–635, thg. 8 2021, doi: 10.1080/10667857.2020.1786781.
[21] R. A. Nugroho *và c.s.*, "Enhanced photo-Fenton degradation of Eosin Y via sonochemical integration of Fe_3O_4 into solvent-free synthesised MIL-100(Cr)", *International Journal of Environmental Analytical Chemistry*, tập 106, số 9, tr 2725–2744, thg. 7 2026, doi: 10.1080/03067319.2025.2588641.
[22] M. Pavlidis, T. Stupp, R. Naskar, C. Cengiz, và S. Thanos, "Retinal Ganglion Cells Resistant to Advanced Glaucoma: A Postmortem Study of Human Retinas with the Carbocyanine Dye DiI", *Invest. Ophthalmol. Vis. Sci.*, tập 44, số 12, tr 5196, thg. 12 2003, doi: 10.1167/iovs.03-0614.
[23] Y. F. Sasaki *và c.s.*, "The comet assay with 8 mouse organs: results with 39 currently used food additives", *Mutation Research/Genetic Toxicology and Environmental Mutagenesis*, tập 519, số 1, tr 103–119, thg. 8 2002, doi: 10.1016/S1383-5718(02)00128-6.
[24] J. D. Sun *và c.s.*, "The inhalation toxicity of two commercial dyes: Solvent Yellow 33 and Solvent Green 3", *Fundamental and Applied Toxicology*, tập 8, số 3, tr 358–371, thg. 4 1987, doi: 10.1016/0272-0590(87)90085-6.
[25] S. Sharma, R. P. Goyal, G. Chakravarty, và A. Sharma, "Toxicity of tomato red, a popular food dye blend on male albino mice", *Experimental and Toxicologic Pathology*, tập 60, số 1, tr 51–57, thg. 6 2008, doi: 10.1016/j.etp.2007.11.005.
[26] J. F. Borzelleca, C. C. Capen, và J. B. Hallagan, "Lifetime toxicity/carcinogenicity study of FD & C Red No. 3 (erythrosine) in rats", *Food and Chemical Toxicology*, tập 25, số 10, tr 723–733, thg. 10 1987, doi: 10.1016/0278-6915(87)90226-2.
[27] G. M. Abd El-Gelil, M. S. Mansour, E. E. Ebrahiem, A. H. EL-Shazly, và H. Abou-Gabal, "Degradation of Eosin Y in Water by Corona Treatment with a Dielectric Barrier Discharge Plasma", *Chemical Engineering & Technology*, tập 43, số 10, tr 2015–2022, 2020, doi: 10.1002/ceat.202000171.
[28] D. Singh, V. S. Kundu, và A. S. Maan, "Structural, morphological and gas sensing study of palladium doped tin oxide nanoparticles synthesized via hydrothermal technique", *Journal of Molecular Structure*, tập 1100, tr 562–569, thg. 11 2015, doi: 10.1016/j.molstruc.2015.08.009.
[29] A. K. Moses, S. R. Tripathy, và S. S. Baral, "Fe-doped SnO_2 nanoparticles: enhancing the photocatalytic hydrogen efficiency, Rhodamine-B dye degradation and visible light absorption", *Mater Renew Sustain Energy*, tập 14, số 1, tr 14, thg. 1 2025, doi: 10.1007/s40243-024-00288-1.
[30] V. H. Huong, V. C. Nguyen, K. P. Pham, T. B. Nguyen, A. B. Ngac, và T. Thi Loan, "Construction dual active sites on SnO_2 via Fe doping for effective ciprofloxacin photodegradation", *Journal of Alloys and Compounds*, tập 1005, tr 176020, thg. 11 2024, doi: 10.1016/j.jallcom.2024.176020.

Mai Khanh Quach received the Bachelor's degree in Chemistry from the University of Science, VNU-HCM, in 2024, and the Master's degree in Inorganic Materials Chemistry from Le Mans Université, France, in 2025. The author is currently a Lecturer at Ho Chi Minh City University of Technology and Engineering, Vietnam. The research interests include inorganic materials, metal oxide nanomaterials, photocatalytic degradation of pollutants.
Email: khanhqm@hcmute.edu.vn. ORCID: https://orcid.org/0009-0004-5511-6040.

Tuyen Nguyen Ngoc Lam is a fourth-year student at the Faculty of Chemistry and Life Sciences, Ho Chi Minh City University of Technology and Engineering in 2025. The major is Inorganic Chemistry.
Email: 22128085@hcmute.edu.vn. ORCID: https://orcid.org/0009-0004-9241-3917.

Nhu Vo Thi Thu received the PhD degree in Chemical Engineering from Ho Chi Minh City University of Technology, Vietnam, in 2020. The author is currently a lecturer at Ho Chi Minh City University of Technology and Engineering. The author has published more than 20 research articles. The research interests are in inorganic materials, nanomaterials, photocatalysis, and environmental applications.
Email: nhuvtt@hcmute.edu.vn. ORCID: https://orcid.org/0000-0002-3587-3819.